mathematics

MDPI

Article

Evaluation of VLBI Observations with Sensitivity and Robustness Analyses

Pakize Küreç Nehbit [1,2,*], Robert Heinkelmann [2], Harald Schuh [2,3], Susanne Glaser [2], Susanne Lunz [2], Nicat Mammadaliyev [2,3], Kyriakos Balidakis [2], Haluk Konak [1] and Emine Tanır Kayıkçı [4]

1 Department of Geomatics Engineering, Kocaeli University, Kocaeli 41001, Turkey; hkonak@kocaeli.edu.tr
2 GFZ German Research Centre for Geosciences, 14473 Potsdam, Germany; robert.heinkelmann@gfz-potsdam.de (R.H.); susanne.glaser@gfz-potsdam.de (S.G.); susanne.lunz@gfz-potsdam.de (S.L.); kyriakos.balidakis@gfz-potsdam.de (K.B.)
3 Chair of Satellite Geodesy, Technische Universität Berlin, 10623 Berlin, Germany; harald.schuh@tu-berlin.de (H.S.); nicat.mammadaliyev@campus.tu-berlin.de (N.M.)
4 Department of Geomatics Engineering, Karadeniz Technical University, Trabzon 61080, Turkey; etanir@ktu.edu.tr
* Correspondence: nehbit@gfz-potsdam.de

Received: 27 April 2020; Accepted: 3 June 2020; Published: 8 June 2020

Abstract: Very Long Baseline Interferometry (VLBI) plays an indispensable role in the realization of global terrestrial and celestial reference frames and in the determination of the full set of the Earth Orientation Parameters (EOP). The main goal of this research is to assess the quality of the VLBI observations based on the sensitivity and robustness criteria. Sensitivity is defined as the minimum displacement value that can be detected in coordinate unknowns. Robustness describes the deformation strength induced by the maximum undetectable errors with the internal reliability analysis. The location of a VLBI station and the total weights of the observations at the station are most important for the sensitivity analysis. Furthermore, the total observation number of a radio source and the quality of the observations are important for the sensitivity levels of the radio sources. According to the robustness analysis of station coordinates, the worst robustness values are caused by atmospheric delay effects with high temporal and spatial variability. During CONT14, it is determined that FORTLEZA, WESTFORD, and TSUKUB32 have robustness values changing between 0.8 and 1.3 mm, which are significantly worse in comparison to the other stations. The radio sources 0506-612, NRAO150, and 3C345 have worse sensitivity levels compared to other radio sources. It can be concluded that the sensitivity and robustness analysis are reliable measures to obtain high accuracy VLBI solutions.

Keywords: very long baseline interferometry; sensitivity; internal reliability; robustness; CONT14

1. Introduction

Very Long Baseline Interferometry (VLBI) is used to measure the arrival time differences of the signals that come from extragalactic radio sources to antennas separated by up to one Earth diameter. The main principle of the VLBI technique is to observe the same extragalactic radio source synchronously with at least two radio telescopes. Global distances can be measured with millimeter accuracy using the VLBI technique [1,2].

In 1967, for the first time, VLBI was used for the detection of light deflection [3,4]. Nowadays, VLBI is a primary technique to determine global terrestrial reference frames and in particular their scale, celestial reference frame, and the Earth Orientation Parameters (EOP), which consist of universal time, and terrestrial and celestial pole coordinates [2]. Since VLBI is the only technique that connects the celestial with the terrestrial reference frames, the technique is fundamentally different from the other space geodetic techniques. The radio sources are objects in the International Celestial Reference Frame (ICRF); however, the antenna coordinates are obtained in the International Terrestrial Reference Frame (ITRF).

As a result of its important role in either the Celestial Reference Frame or the Terrestrial Reference Frame, it is essential to investigate the quality of VLBI observations and its effect on the unknown parameters. For this reason, the quality of the VLBI observations was investigated according to sensitivity and robustness criteria. Although robustness and sensitivity criteria are not new methods in geodesy, they have been applied to the VLBI observations for the first time in this study. The location of the weak stations and radio sources were easily detected using sensitivity and robustness criteria. Using reliability criteria allows detecting observations that have undetectable gross errors on the unknown parameters. Besides, investigation of the sensitivity of the network against the outliers plays a crucial role in the improvement of accuracy. In this way, the scheduling can be improved using this method in the future.

Sensitivity criteria have been an inspiration for many scientific investigations. The criteria can be explained as the network capability for the monitoring of crustal movements and deformations [5]. So far, mostly geodetic networks based on GPS measurements have been analyzed: sensitivity levels were determined in [6], the datum definition was investigated using sensitivity in [7], a priori sensitivity levels were computed in [8], and the determination of the experimental sensitivity capacities was examined in [9].

Robustness criteria were developed as a geodetic network analysis alternative to standard statistical analysis in [10]. Robustness analysis is the combination of the reliability analysis introduced in [11] and the geometrical strength analysis. Robustness has been the main topic of many studies until today. Different strain models were defined with homogeneous and heterogeneous deformation models in [12]. The displacement vectors defined the effect of the undetectable gross error on the coordinate unknowns, which was determined independently from the translation in [13]. In addition, to obtain the corrected displacement vector, global initial conditions represented by the whole station network were used. Local initial conditions aiming at minimizing the total displacement were developed for the polyhedron represented by each network point as defined in [14].

The paper is organized as follows. Section 2 presents the theoretical background of the sensitivity analysis in the VLBI network. Section 3 introduces the theoretical background of robustness. Section 4 investigates the sensitivity and robustness levels of the VLBI network observed during the continuous campaign CONT14, a continuous VLBI session, which will be further described in Section 4. There, 15 VLBI sessions were evaluated, and the outliers were detected using the software VieVS@GFZ (G2018.7, GFZ, Potsdam, Germany) [15], a fork from the Vienna VLBI Software [16]. The least-squares adjustment module of the VieVS@GFZ software was modified to determine the sensitivity levels of the stations and the radio sources and to obtain the robustness level of the observing stations. The sensitivity levels of the stations and the radio sources were obtained using the developed module for the 15 24-h sessions. The computed sensitivity levels of the stations and radio sources were compared session by session. In addition, the deformation resistance induced by the maximum undetectable errors with the internal reliability analysis was computed for each session. The obtained displacement vectors were compared with threshold values. Conclusions and recommendations for further research will be provided in Section 5.

2. The Sensitivity in the VLBI Network

Sensitivity is the minimum value of undetectable gross errors in the adjusted coordinate differences. The sensitivity levels give information about the weakness of a network. The sensitivity level is computed using the cofactor matrix of the displacement vector estimated from two different sessions.

Using the adjusted coordinates $\hat{\boldsymbol{x}}^1$, $\hat{\boldsymbol{x}}^2$ and their cofactor matrices $\boldsymbol{Q}_{xx}^1, \boldsymbol{Q}_{xx}^2$ based on different sessions 1 and 2, the displacement vector ($\boldsymbol{d}$) and the corresponding cofactor matrix ($\boldsymbol{Q}_{dd}$) for one point (reference point of a station or radio source) are obtained using the following equations:

$$\boldsymbol{d} = \widehat{\boldsymbol{x}}^1 - \widehat{\boldsymbol{x}}^2 \tag{1}$$

$$\boldsymbol{Q}_{dd} = \boldsymbol{Q}_{xx}^1 + \boldsymbol{Q}_{xx}^2. \tag{2}$$

Alternatively, when it is aimed to obtain the sensitivity level of each session as a priori sensitivity level, the cofactor matrix of the displacement vector is obtained as $\boldsymbol{Q}_{dd} = \boldsymbol{Q}_{xx}$ [9,14] and the weight matrix of the displacement vector for each station $\boldsymbol{P}_{d_i}$ is computed by the following equations

$$\begin{bmatrix} \boldsymbol{d}_1 \\ \boldsymbol{d}_2 \\ \cdot \\ \boldsymbol{d}_n \end{bmatrix} = \begin{bmatrix} \boldsymbol{N}_{11} & \boldsymbol{N}_{12} & \cdot & \boldsymbol{N}_{1n} \\ \boldsymbol{N}_{21} & \boldsymbol{N}_{22} & \cdot & \boldsymbol{N}_{2n} \\ \cdot & \cdot & \cdot & \cdot \\ \boldsymbol{N}_{n1} & \boldsymbol{N}_{n2} & \cdot & \boldsymbol{N}_{nn} \end{bmatrix}^+ \begin{bmatrix} (\boldsymbol{A}^T\boldsymbol{Pdl})_1 \\ (\boldsymbol{A}^T\boldsymbol{Pdl})_2 \\ \cdot \\ (\boldsymbol{A}^T\boldsymbol{Pdl})_n \end{bmatrix} \tag{3}$$

$$\boldsymbol{d}_i = \begin{bmatrix} dx_i \\ dy_i \\ dz_i \end{bmatrix} = \ddot{\boldsymbol{N}}_i \boldsymbol{A}^T \boldsymbol{Pdl} \tag{4}$$

$$\boldsymbol{Q}_{d_i d_i} = \ddot{\boldsymbol{N}}_i \boldsymbol{A}^T \boldsymbol{P} \boldsymbol{Q}_{ll} \boldsymbol{P} \boldsymbol{A} \ddot{\boldsymbol{N}}_i^T = \ddot{\boldsymbol{N}}_i \boldsymbol{N} \ddot{\boldsymbol{N}}_i^T \tag{5}$$

$$\boldsymbol{P}_{d_i} = \left(\boldsymbol{Q}_{d_i d_i}\right)^{-1} \tag{6}$$

where i= *1, ..,n* is the number of stations, $\boldsymbol{A}$ is the design matrix, $\boldsymbol{P}$ is the weight matrix, $\boldsymbol{N}$ is the normal equation system, $\boldsymbol{A}^T\boldsymbol{Pdl}$ is the right-hand side vector, $\boldsymbol{Q}_{ll}$ is the cofactor matrix of the observations, $\boldsymbol{d}_i$ is the displacement vector at the i^{th} station, $\boldsymbol{P}_{d_i}$ is the weight matrix of the displacement vector at the i^{th} station, and $\ddot{\boldsymbol{N}}_i$ is the sub-matrix of the normal equation system for the i^{th} station.

The obtained weight matrix $\boldsymbol{P}_{d_i}$ is decomposed into its eigenvalue and eigenvector. The minimum detectable displacement value—namely, the best sensitivity level (d_{min})—depends on the inverse of the maximum eigenvalue of the weight matrix (λ_{max}) for each station

$$\|d\|_{min} = \frac{W_0 \sigma}{\sqrt{\lambda_{max}}} \tag{7}$$

where σ is derived from the theoretical variance of the unit weight [6] and the threshold value of the non-centrality parameter (W_0) is determined through $W_0 = W(\alpha_0, \gamma_0, h, \infty)$ based on the power of the test $\gamma_0 = 80\%$, the significance level $\alpha_0 = 5\%$, and the degree of freedom $h = 1$ [17,18].

With single-session VLBI analysis, station and radio source coordinates, clock parameters, pole coordinates, and Universal Time 1 (UT1) minus Universal Time Coordinated (UTC), celestial pole coordinates, and atmosphere parameters can be determined [2,19]. To evaluate the VLBI observations, the mathematical model of the least-squares adjustment is expanded by the matrix of constraints $\boldsymbol{H}$. The functional model for the actual observations $\boldsymbol{l}$ and constraint parameters $\boldsymbol{l_h}$ can be written as follows:

$$\boldsymbol{v} = \boldsymbol{Ax} - \boldsymbol{l} \tag{8}$$

$$\boldsymbol{v}_c = \boldsymbol{Hx} - \boldsymbol{l_h} \tag{9}$$

where $\boldsymbol{v}$ is the residual vector, $\boldsymbol{v}_c$ is the residual vector of constraints, and $\boldsymbol{x}$ denotes the vector of the unknown parameters [20]. Accordingly, the functional model of the adjustment can be summarized with the following symbolic equations:

$$\begin{bmatrix} \boldsymbol{v} \\ \boldsymbol{v}_c \end{bmatrix} = \begin{bmatrix} \boldsymbol{A} \\ \boldsymbol{H} \end{bmatrix} \boldsymbol{x} - \begin{bmatrix} \boldsymbol{l} \\ \boldsymbol{l_h} \end{bmatrix} \tag{10}$$

and the corresponding stochastic model of the adjustment is written as:

$$\boldsymbol{P} = \begin{bmatrix} \boldsymbol{P}_{ll} & \\ & \boldsymbol{P}_c \end{bmatrix} \tag{11}$$

where $\boldsymbol{P}_{ll}$ is the weight matrix of the actual observations, $\boldsymbol{P}_c$ is the weight matrix of the constraint parameters, and the remaining elements of this block-diagonal matrix are equal to zero. According to the adjustment model, the cofactor matrix of the unknown parameters is determined as:

$$\boldsymbol{Q}_{xx} = (\boldsymbol{A}^T\boldsymbol{P}\boldsymbol{A} + \boldsymbol{H}^T\boldsymbol{P}_c\boldsymbol{H})^{-1} \tag{12}$$

where $\boldsymbol{Q}_{xx}$ covers all unknown parameters of the respective VLBI session.

Using the functional and the stochastic models, the unknown parameters are computed with a free network adjustment. The cofactor matrix of the displacement vector of each station is as follows

$$\boldsymbol{Q}_{xx} = \begin{bmatrix} \cdot & \cdot & \cdot & \cdot & \cdot & \cdot & \cdot & \cdot & \cdot & \cdot \\ \cdot & \cdot & q_{x1x1} & q_{x1x2} & q_{x1y1} & q_{x1y2} & q_{x1z1} & q_{x1z2} & \cdot & \cdot \\ \cdot & \cdot & q_{x2x1} & q_{x2x2} & q_{x2y1} & q_{x2y2} & q_{x2z1} & q_{x2z2} & \cdot & \cdot \\ \cdot & \cdot & q_{y1x1} & q_{y1x2} & q_{y1y1} & q_{y1y2} & q_{y1z1} & q_{y1z2} & \cdot & \cdot \\ \cdot & \cdot & q_{y2x1} & q_{y2x2} & q_{y2y1} & q_{y2y2} & q_{y2z1} & q_{y2z2} & \cdot & \cdot \\ \cdot & \cdot & q_{z1x1} & q_{z1x2} & q_{z1y1} & q_{z1y2} & q_{z1z1} & q_{z1z2} & \cdot & \cdot \\ \cdot & \cdot & q_{z2x1} & q_{z2x2} & q_{z2y1} & q_{z2y2} & q_{z2z1} & q_{z2z2} & \cdot & \cdot \\ \cdot & \cdot & \cdot & \cdot & \cdot & \cdot & \cdot & \cdot & \cdot & \cdot \end{bmatrix}_{u,u} \tag{13}$$

where u is the number of unknown parameters. For the first station, the matrix $\ddot{\boldsymbol{N}}_i$ is determined as

$$\ddot{\boldsymbol{N}}_1 = \begin{bmatrix} \cdot\cdot & \cdot\cdot & \cdot\cdot & q_{x1x1} & q_{x1x2} & q_{x1y1} & q_{x1y2} & q_{x1z1} & q_{x1z2} \\ \cdot\cdot & \cdot\cdot & \cdot\cdot & q_{y1x1} & q_{y1x2} & q_{y1y1} & q_{y1y2} & q_{y1z1} & q_{y1z2} \\ \cdot\cdot & \cdot\cdot & \cdot\cdot & q_{z1x1} & q_{z1x2} & q_{z1y1} & q_{z1y2} & q_{z1z1} & q_{z1z2} \end{bmatrix}_{3,u} \tag{14}$$

and the cofactor matrix of the displacement vector of the first station is obtained as

$$\left(\boldsymbol{Q}_{d_1d_1}\right)_{3,3} = \ddot{\boldsymbol{N}}_1\boldsymbol{N}\ddot{\boldsymbol{N}}_1^T = \begin{bmatrix} q_{x1x1} & q_{x1y1} & q_{x1z1} \\ q_{y1x1} & q_{y1y1} & q_{y1z1} \\ q_{z1x1} & q_{z1y1} & q_{z1z1} \end{bmatrix}_{3,3}. \tag{15}$$

In analogy, for each radio source, the cofactor matrix of the displacement vector is obtained using the following equations

$$\boldsymbol{Q}_{xx} = \begin{bmatrix} \cdot & \cdot & \cdot & \cdot & \cdot & \cdot \\ \cdot & q_{\alpha1\alpha1} & q_{\alpha1\alpha2} & q_{\alpha1\delta1} & q_{\alpha1\delta2} & \cdot \\ \cdot & q_{\alpha2\alpha1} & q_{\alpha2\alpha2} & q_{\alpha2\delta1} & q_{\alpha2\delta2} & \cdot \\ \cdot & q_{\delta1\alpha1} & q_{\delta1\alpha2} & q_{\delta1\delta1} & q_{\delta1\delta2} & \cdot \\ \cdot & q_{\delta2\alpha1} & q_{\delta2\alpha2} & q_{\delta2\delta1} & q_{\delta2\delta2} & \cdot \\ \cdot & \cdot & \cdot & \cdot & \cdot & \cdot \end{bmatrix}_{u,u}. \tag{16}$$

α and δ are the source equatorial coordinates defined as right ascension and declination, respectively, and u is defined as above. For the first radio source, the matrix $\ddot{\boldsymbol{N}}_i$ is determined as

$$\ddot{\boldsymbol{N}}_1 = \begin{bmatrix} \cdot & \cdot & q_{\alpha1\alpha1} & q_{\alpha1\alpha2} & q_{\alpha1\delta1} & q_{\alpha1\delta2} & \cdot & \cdot \\ \cdot & \cdot & q_{\delta1\alpha1} & q_{\delta1\alpha2} & q_{\delta1\delta1} & q_{\delta1\delta2} & \cdot & \cdot \end{bmatrix}_{2,u} \tag{17}$$

and the cofactor matrix of the displacement vector of the first radio source is

$$\left(\boldsymbol{Q}_{d_1d_1}\right)_{2,2} = \ddot{\boldsymbol{N}}_1\boldsymbol{N}\ddot{\boldsymbol{N}}_1^T = \begin{bmatrix} q_{\alpha1\alpha1} & q_{\alpha1\delta1} \\ q_{\delta1\alpha1} & q_{\delta1\delta1} \end{bmatrix}_{2,2}. \tag{18}$$

Subsequently, the corresponding weight matrix belonging to each station or radio source is computed as shown in Equation (6), and the minimum value of the undetectable gross errors is found by Equation (7).

3. The Robustness of VLBI Stations

Robustness is defined as a function of the reliability criteria [10]. On the other hand, the robustness of a geodetic network is defined as the strength of deformation caused by undetectable gross errors with the internal reliability analysis. The robustness analysis consists of enhancing the internal reliability analysis with the strain technique [10,21].

Internal reliability can be interpreted as the controlling of an observation via the other observations in a network. It can be quantified as the magnitude of the undetectable gross errors by using hypothesis testing. For correlated observations, the internal reliability of the j^{th} observation is obtained with the following equations:

$$\Delta_{0j} = m_0 \sqrt{\frac{W_0}{\boldsymbol{e}_j^T \boldsymbol{P} \boldsymbol{Q}_{\hat{v}\hat{v}} \boldsymbol{P} \boldsymbol{e}_j}} \quad (19)$$

$$\boldsymbol{e}_j^T = [.. \quad 0 \quad 0 \quad 1 \quad 0 \quad ...] \quad (20)$$

where m_0 is derived from the a posteriori value of the experimental variance, $\boldsymbol{Q}_{\hat{v}\hat{v}}$ is the cofactor matrix of the residuals, $\boldsymbol{e}_j^T$ is a selection vector, which consists of 1 for the j^{th} observation and 0 for the other observations; its dimension equals the total number of observations.

The robustness of each VLBI station is quantified as the effect of the maximal undetectable gross error on the coordinate unknowns ($\Delta\boldsymbol{x}$) [10,13,22] as

$$\Delta\boldsymbol{x} = \boldsymbol{Q}\boldsymbol{A}^T\boldsymbol{P}\Delta_{0j} \quad (21)$$

$$\Delta_{0j}{}^T = [.. \quad 0 \quad 0 \quad \delta_{0j} \quad 0 \quad ...] \quad (22)$$

where $\Delta_{0j}{}^T$ is a vector, which consists of the internal reliability value of the j^{th} observation and 0 for the other observations, with the dimensions of the total number of observations. The displacement vector can be written as

$$\Delta\boldsymbol{x}_i = \begin{bmatrix} \Delta x_i \\ \Delta y_i \\ \Delta z_i \end{bmatrix} = \begin{bmatrix} u_i \\ v_i \\ w_i \end{bmatrix} \quad (23)$$

where u_i, v_i, and w_i are the displacement vector components in the x-, y-, and z-directions.

$$\Delta\boldsymbol{x}_i^T = \left[\Delta\boldsymbol{x}_1;\ \Delta\boldsymbol{x}_2;\ \ldots\ldots\ldots\ldots\ldots;\ \Delta\boldsymbol{x}_j\right] \quad (24)$$

The effect of the undetected gross error on the unknown coordinate is calculated for any coordinate unknown. The effect can be obtained many times using each observation for any coordinate unknown. Each observation causes strain with different magnitude and direction. For this reason, the observation having maximum effect on the coordinate unknowns must be identified

$$\Delta\boldsymbol{x}_{0j} = max\{\|\Delta x_j\|\}. \quad (25)$$

It is supposed that the observation having a maximum vector norm causes maximum strain. To compute the vector norm of each observation, the L1 norm is used as

$$\|\Delta x_j\| = |\Delta x_1| + |\Delta x_2| + \cdots + |\Delta x_u| \quad (26)$$

where u is the number of unknowns.

For the strain computation, the surface formed by the station and its neighboring stations, which are connected through baselines, is used. The strain resulting from the effect of the undetectable gross errors on the coordinate unknowns can be obtained for the polyhedron represented by each network point, with affine or extended Helmert transformation models [14,22].

The displacement vector related to the strain parameters can be determined with the equations:

$$\begin{bmatrix} \Delta x_i \\ \Delta y_i \\ \Delta z_i \end{bmatrix} = \boldsymbol{E}_i \begin{bmatrix} X_i - X_0 \\ Y_i - Y_0 \\ Z_i - Z_0 \end{bmatrix} \quad (27)$$

$$\boldsymbol{E}_i = \begin{bmatrix} \frac{\partial u}{\partial x} & \frac{\partial u}{\partial y} & \frac{\partial u}{\partial z} \\ \frac{\partial v}{\partial x} & \frac{\partial v}{\partial y} & \frac{\partial v}{\partial z} \\ \frac{\partial w}{\partial x} & \frac{\partial w}{\partial y} & \frac{\partial w}{\partial z} \end{bmatrix} = \begin{bmatrix} e_{xx} & e_{xy} & e_{xz} \\ e_{yx} & e_{yy} & e_{yz} \\ e_{zx} & e_{zy} & e_{zz} \end{bmatrix} \quad (28)$$

where $\boldsymbol{E}_i$ is the strain tensor, X_0, Y_0, and Z_0 are the initial conditions, X_i, Y_i, and Z_i are the coordinate unknowns of the i^{th} station located on the surface, e_{xx} is the rate of change in the x-direction with respect to the position component in the x-direction [12].

The strain parameters are independent of the location of surfaces in the coordinate system. For this reason, at each surface, the strain tensor is computed with a reference point P_0 selected on the surface. Using the obtained strain tensor, the objective function is linearized according to the initial conditions via

$$\sum_{i=1}^{n}(\Delta\boldsymbol{x})^T\boldsymbol{E}_i^T\boldsymbol{E}_i(\Delta\boldsymbol{x}) \rightarrow min \tag{29}$$

$$\sum_{i=1}^{n}\boldsymbol{E}_i^T\boldsymbol{E}_i(\boldsymbol{X}_i-\boldsymbol{X}_0) = 0 \tag{30}$$

$$-\sum_{i=1}^{n}\boldsymbol{E}_i^T\boldsymbol{E}_i\boldsymbol{X}_0 + \sum_{i=1}^{n}\boldsymbol{E}_i^T\boldsymbol{E}_i\boldsymbol{X}_i = 0 \tag{31}$$

where the initial conditions $\boldsymbol{X}_0^T = [X_0 \quad Y_0 \quad Z_0]$ are computed as follows

$$\boldsymbol{X}_0 = \left[\sum_{i=1}^{n}\boldsymbol{E}_i^T\boldsymbol{E}_i\right]^{-1}\sum_{i=1}^{n}\boldsymbol{E}_i^T\boldsymbol{E}_i\boldsymbol{X}_i. \tag{32}$$

When inserting these initial conditions into Equation (27), the corrected displacement vector is obtained [13]. In other words, the displacement vector is translated to the gravity center of the surface computed as:

$$d_i = \sqrt{u_i^2 + v_i^2 + w_i^2}. \tag{33}$$

If the corrected displacement vector is estimated from the surface represented by the whole network of stations, the corrected global displacement vector is obtained. However, if the corrected displacement vector is estimated from the surface represented by each station, local initial conditions (X_{L0}) are obtained as

$$\boldsymbol{X}_{L0} = (\boldsymbol{E}_i^T\boldsymbol{E}_i)^{-1}\boldsymbol{E}_i^T\boldsymbol{E}_i\sum_{i=1}^{m}\boldsymbol{X}_i \tag{34}$$

where m is the number of stations that have a baseline to the i^{th} station. Using the local initial conditions, the corrected local displacement vector is computed via Equation (27). The computed magnitudes of the displacement vectors are compared with the threshold value estimated from confidence ellipsoids [23]:

$$W_i = m_0\sqrt{3F_{h,f,1-\alpha_0}trace(\boldsymbol{Q}_{xx})} \tag{35}$$

where f is the degree of freedom, and α_0 is the significance level.

In case of $d_i > W_i$, we conclude that the network station is not robust [13]. In other words, the network is not sensitive enough to possible outliers and their disturbing effects on the coordinate unknowns.

Due to the fact that the displacement vectors obtained for any station represent the effect of undetectable errors on the coordinate unknowns [14,22], the displacement vectors can be compared to the sensitivity levels d_{min} as well.

4. Results

In order to compare VLBI stations and radio sources approximately under the same conditions, such as scheduling and station geographical distribution, we selected the continuous VLBI Campaign

2014 (CONT14) (https://ivscc.gsfc.nasa.gov/program/cont14) for the numerical test. CONT14 consists of 15 continuous VLBI sessions observed from 2014-May-6, 00:00 UT to 2014-May-20, 23:59 UT. The observations of CONT14 were evaluated session by session with the software VieVS@GFZ written in MatLab©.

To obtain the sensitivity levels of the radio sources and stations, Equations (6), (7), and (13)–(18) mentioned in Section 2 and, to obtain the robustness values of the network stations, Equations (19)–(26) mentioned in Section 3 were added to the least-squares adjustment module in VieVS@GFZ.

In order to obtain the strain parameters on the surfaces, displacement vector components and observed baselines were computed with a small C++ program for each session. According to the strain parameters, magnitudes of the corrected local and global displacement vectors were determined for each station and compared with the threshold values.

4.1. Results of the Sensitivity Analysis

The sensitivity level of a station reflects the total observation weights of the station and the remoteness of the station in the network. A small sensitivity value indicates that a station is strongly controlled by the other stations and hence, its sensitivity level is better.

According to the sensitivity analysis of the CONT14 campaign, the subset of European stations, ONSALA60, WETTZELL, ZELENCHK, MATERA, YEBES40M, and partly NYALES20 have the best sensitivity levels based on all sessions, whereas BADARY provides the worst sensitivity level based on all sessions (Figure 1). Across the sessions, there are small but significant differences as well.

The sensitivity levels of the radio sources show that some radio sources in individual sessions have orders of magnitude larger sensitivity levels, e.g., NRAO150, 3C345, 3C454.3, and 0506-612 (Figure 2).

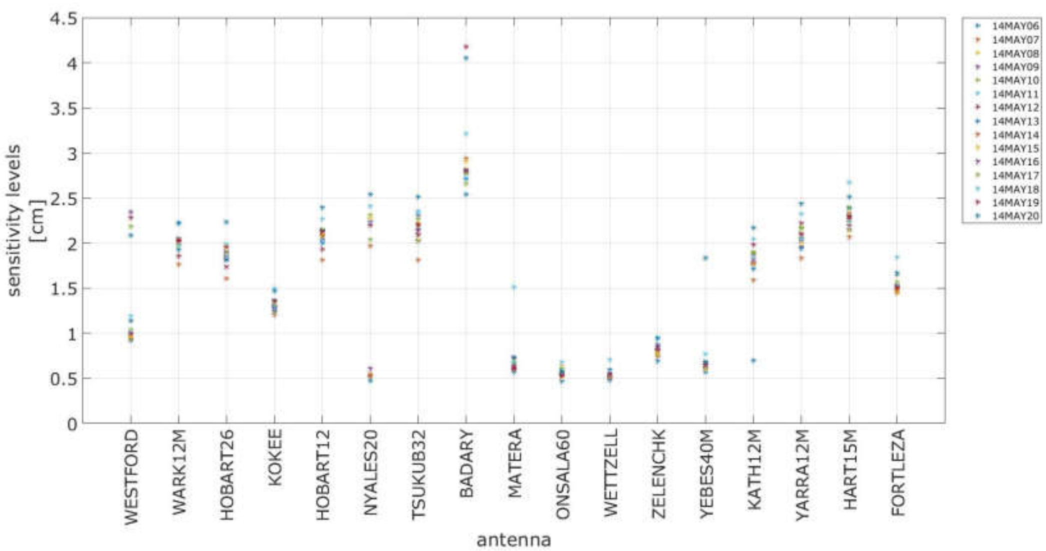

Figure 1. The sensitivity level distributions of the antennas in continuous VLBI Campaign 2014 (CONT14). On the horizontal axis, the antennas are displayed in their respective order of appearance, i.e., unsorted.

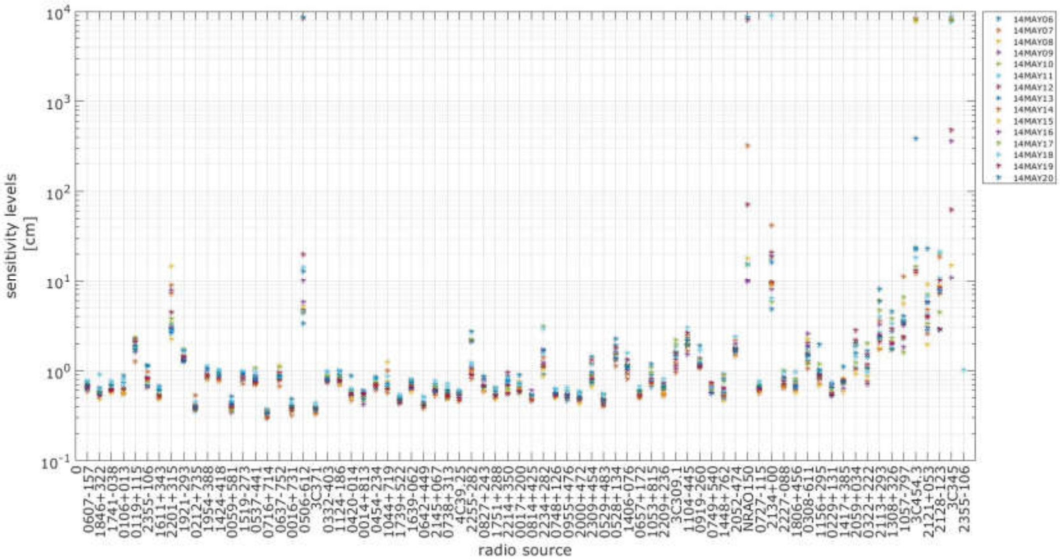

Figure 2. The sensitivity distributions of the radio sources in CONT14. Sources appear randomly on the horizontal axis.

4.2. Result of the Robustness Analysis

The robustness of the network is computed based on the internal reliability and reflects the maximum effect of the undetectable gross error on the coordinate unknowns. In well-designed geodetic networks, the internal reliability value of the observations can be expected below $8m_i$, which is defined as the average error of the observations [8,24–27].

In each session, all observations were tested regarding whether they have gross errors. After the outliers were detected and removed from the observation list, the internal reliability of the observations was investigated.

In Figure 3, some internal reliability values with very large magnitudes can be easily identified. To investigate the large internal reliability magnitudes, the radio sources (and baselines) involved in the observations were identified (Table 1). Comparing the findings to the sensitivity of the radio sources, it could be seen that these radio sources also had the worst sensitivity magnitudes.

If an acceptable mathematical model is used for the adjustment, the statistical analyses can be obtained confidently. For this reason, internal reliability and sensitivity analysis should be performed for all observations.

After all observations of the radio sources mentioned in Table 1 were excluded, it was found that the remaining internal reliabilities fell into a significantly smaller range in Figure 4 compared to Figure 3. Using the outlier-free radio source list, the sensitivity level of the radio sources was obtained. It is seen that radio source 3C454.3 has the maximum sensitivity level (Figure 5). In order to investigate the robustness of the stations with best quality observations, the radio sources having the worst sensitivity levels were excluded. When the observations are reduced according to both internal reliability and the sensitivity levels, the internal reliability criteria can be obtained for the well-designed network.

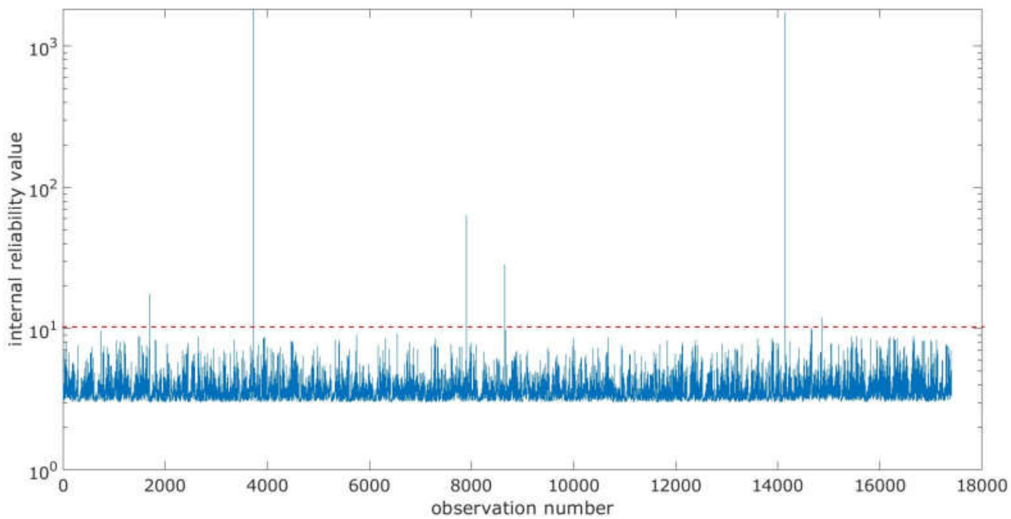

Figure 3. Internal reliability values of the observations in session 14MAY08XA (CONT14) (observations exceeding the red line were identified as outliers and excluded).

Table 1. Observations with largest internal reliability values in session 14MAY08XA.

Session	Observation Number	Internal Reliability	Baseline	Radio Source
14MAY08XA	3735	1.83×10^3	MATERA-YEBES40M	NRAO150 (0355+508)
	14,144	1.71×10^3	MATERA-ZELENCHK	3C345 (1641+399)
	7903	6.35×10^1	ONSALA60-ZELENCHK	2134+00 (2134+004)
	1702	1.75×10^1	FORTLEZA-HART15M	1057−797
	8661	2.83×10^1	WESTFORD-FORTLEZA	2128−123
	14,855	1.18×10^1	KATH12M-YARRA12M	0506−612

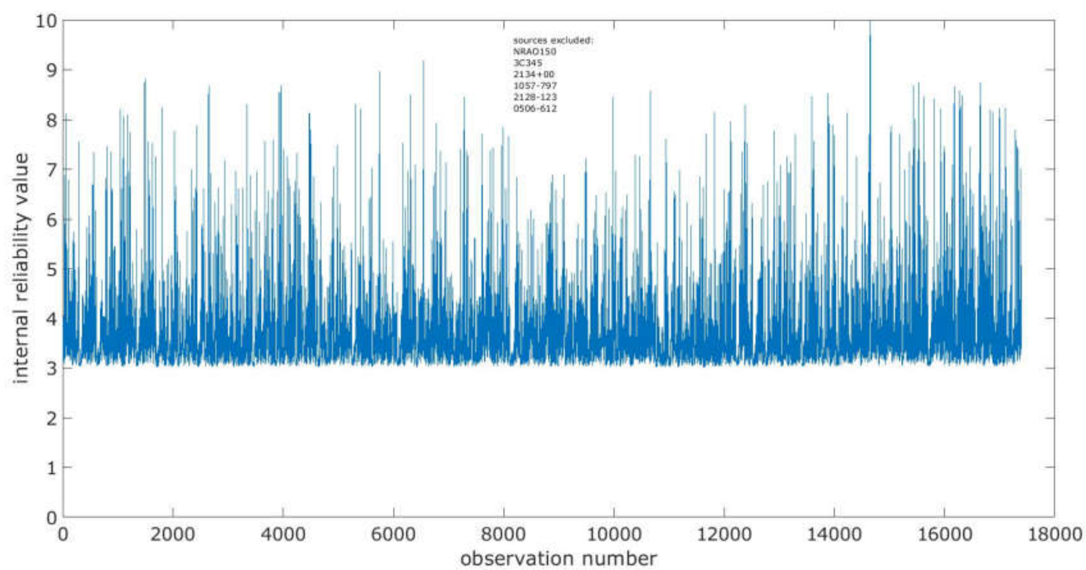

Figure 4. Internal reliability values of the outlier-free observations in session 14MAY08XA.

After this step, the robustness values of the stations were computed. For this purpose, the observation having maximum effect on the coordinate unknowns in each session was selected for the robustness analysis. According to Table 2, it is clearly seen in all sessions that the FORTLEZA station is affected. Table 2 also displays the radio sources that were involved in the observations affecting FORTLEZA. However, the radio sources are identified as rather compact sources because of their small CARMS (closure amplitude rms) values based on natural weighting [28], which are below 0.4.

As mentioned above, the maximum effect of undetected gross error on the station coordinates is called a displacement vector, and it was computed using Equation (21) for CONT14. According to the obtained displacement vector components for CONT14, the magnitudes of the displacement vector components in both x and y directions are about the same but with a different sign, whereas the magnitude in the z direction is about one order of magnitude smaller. In all sessions, FORTLEZA is the most affected one due to undetected gross errors. If we focus on the motion of FORTLEZA during CONT14, the x component of the displacement vector was found to be about between 2 and 4 mm (Figure 6).

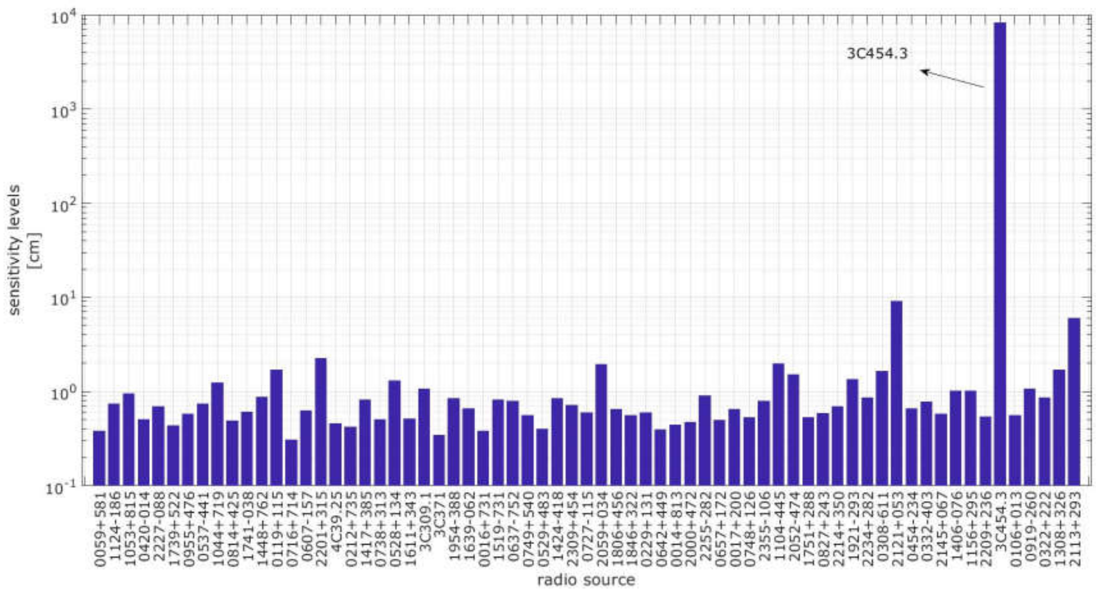

Figure 5. The sensitivity distribution of the radio sources after outlier elimination in session 14MAY08XA.

In each session, the robustness of the stations was obtained with the displacement vector components. To obtain the strain parameters, the surface that was used consists of the station and its neighboring stations connected through baselines. The strain parameters were computed using Equation (27) for the surface that contains each antenna. Using the strain parameters computed for all surfaces represented by the stations, the local displacement vectors were translated according to the gravity center of the surfaces with Equations (27) and (34). The distributions of the local displacement vector magnitudes are illustrated in Figure 7 for one session only: 14MAY08XA.

Table 2. List of observations with a maximum effect of the undetectable gross error on the station coordinates distribution during CONT14.

Session	Observation Number	Baseline	Baseline Length (km)	Affected Station	Radio Source	CARMS Nat. Weight. [28]
14MAY06XA	8973	FORTLEZA-ZELENCHK	8649	FORTLEZA	0454−234	0.17
14MAY07XA	2370	FORTLEZA-HART15M	7025	FORTLEZA	1057−797	0.20
14MAY08XA	13,887	FORTLEZA-WESTFORD	5897	FORTLEZA	0119+115	0.24
14MAY09XA	2207	FORTLEZA-HART15M	7025	FORTLEZA	1057−797	0.20
14MAY10XA	14,313	FORTLEZA-HART15M	7025	FORTLEZA	1424−418	0.18
14MAY11XA	12,560	FORTLEZA-HART15M	7025	FORTLEZA	1424−418	0.18
14MAY12XA	9264	FORTLEZA-HART15M	7025	FORTLEZA	0727−115	0.14
14MAY13XA	15,509	FORTLEZA-WESTFORD	5897	FORTLEZA	0420−014	0.21
14MAY14XA	6772	FORTLEZA-TSUKUB32	12252	FORTLEZA	1611+343	0.36
14MAY15XA	16,477	FORTLEZA-HART15M	7025	FORTLEZA	1751+288	0.18
14MAY16XA	8241	FORTLEZA-HART15M	7025	FORTLEZA	0454−234	0.17
14MAY17XA	5831	FORTLEZA-HART15M	7025	FORTLEZA	0308−611	0.40
14MAY18XA	14,080	FORTLEZA-KATH12M	12553	FORTLEZA	1424−418	0.18
14MAY19XA	1746	FORTLEZA-HART15M	7025	FORTLEZA	1057−797	0.20
14MAY20XA	35	FORTLEZA-WETSFORD	5897	FORTLEZA	0727−115	0.14

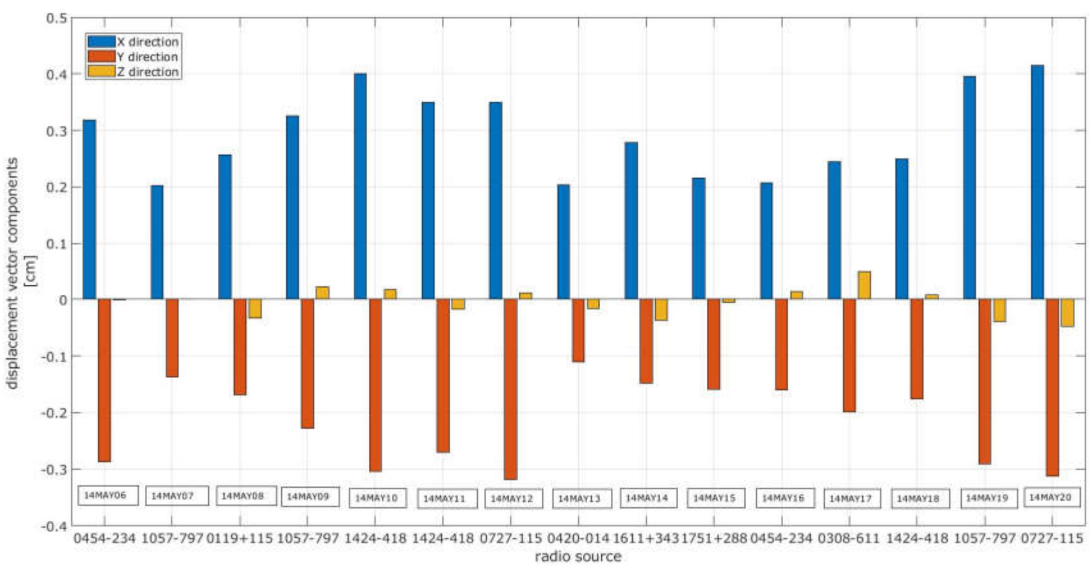

Figure 6. The effect of the undetectable gross errors on station coordinates of FORTLEZA.

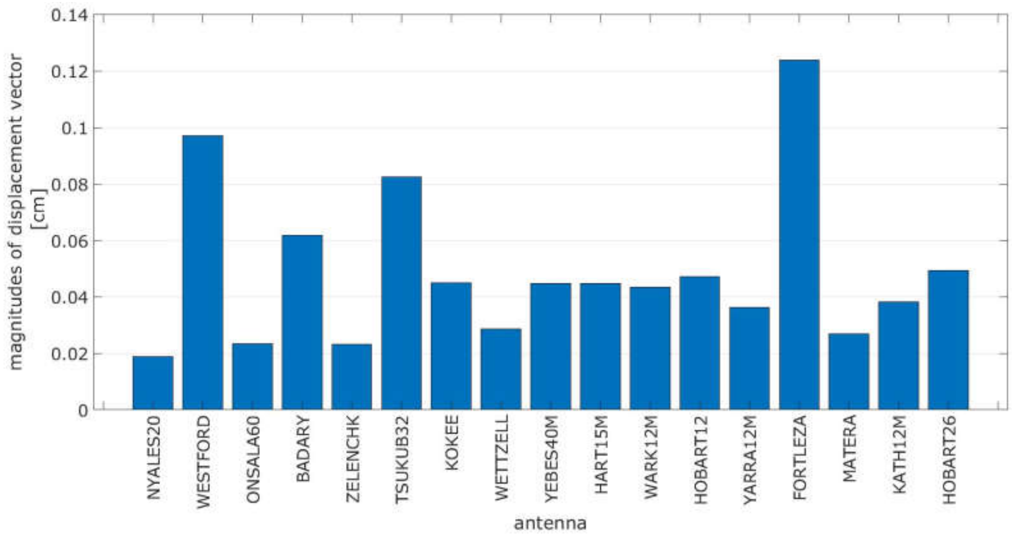

Figure 7. Distribution of local displacement vector magnitudes for Very Long Baseline Interferometry (VLBI) antennas in session 14MAY08XA.

According to Figure 7, FORTLEZA, WESTFORD, and TSUKUB32 have the largest displacement vector magnitudes ranging between 0.8 and 1.3 mm. It can be easily seen that these antennas are affected by the observation having the maximum effect of the undetectable gross errors on the station coordinates.

To address the robustness of the antennas, the computed local displacement vector values were compared to the threshold values obtained applying Equation (35) and the sensitivity levels of the stations as obtained with Equation (7). It was found that all the stations are robust against undetectable gross errors, since the magnitudes of the local displacement vectors are smaller than the threshold values (Figure 8).

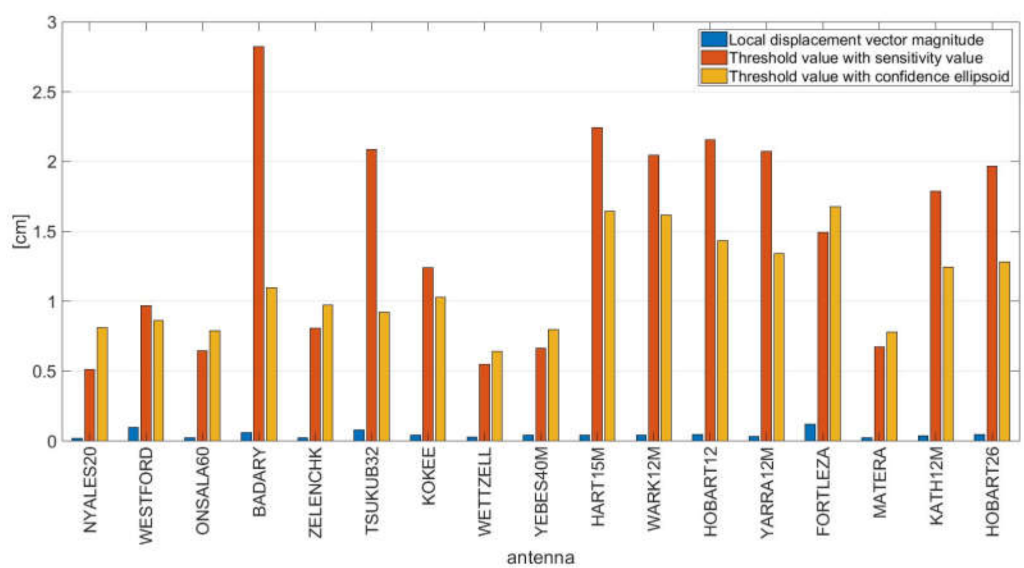

Figure 8. Robustness analysis for VLBI stations in session 14MAY08XA.

5. Discussion

In an astronomical aspect, the structure of the radio sources can cause errors [29], and the astrometric quality of the radio sources is defined by the structure index. Sources with an X-band index of 1 or 2 and S-band index of 1 can be considered as sources of the best astrometric quality. Furthermore, it is recommended that sources with an X-band index of 3 or 4 should not be used [30]. Besides that, previous studies indicate that source structure is a major error source in geodetic VLBI [31]. Sources such as 3C345, 2128−123, and 2134+004 having observations with larger internal reliability values compared to the other sources have a structure index (http://bvid.astrophy.u-bordeaux.fr/) of 4.13, 4.56, and 3.73, respectively, in the X-band. In addition, radio source NRAO150 with a structure index of 2.06 in the S-band has also observations with larger internal reliability. If the radio sources are compared in the view of their sensitivity levels and structure indices, it can be easily understood that the radio source 3C454.3 having a larger sensitivity level has a structure index of 2.9 in the S-band and of 3.84 in the X-band. The radio source 3C454.3 is defined as a quasi-stellar object (QSO) with a core-jet structure that elongates toward the west and bends toward the north-west.

In the robustness analysis, an observation having a maximum effect on the coordinate unknowns more seriously affects those stations used for observing it and their neighboring stations connected with baselines than the other stations in the network. For this reason, network geometry and observation plans are substantial for the robustness analysis. According to the result of the robustness analysis, the observation on the FORTLEZA–WESTFORD baseline has a maximum effect on the coordinate unknowns. In other words, larger magnitudes of the displacement vectors at these stations are obtained. As a result, both FORTLEZA and WESTFORD stations have larger robustness values. In addition, because of the network geometry and the observation plan, TSUKUB32 has larger robustness value than the other stations.

Although the selection of CONT14 is convenient for an initial analysis, the measurements may have systematic errors that cannot be detected in the error analysis because of the short duration of the campaign. Therefore, sensitivity levels of the antennas and the radio sources and robustness values of VLBI antennas may be determined too optimistically.

According to our results, the internal reliability values of the observations and the sensitivity levels of the sources can be used to investigate the source quality together with the structure index. The sources can be excluded based on their sensitivity levels and structure indices. For this reason, it can be considered that robustness and sensitivity criteria can play a substantial role in scheduling in the future.

The software VieVS@GFZ was modified to determine the sensitivity levels and to detect the observations that are having a maximum effect on the coordinate unknowns. It can be used easily for routine analysis of VLBI sessions. However, to obtain the strain parameters and the robustness analysis, VieVS@GFZ should be further modified in the future.

6. Conclusions

In this research, we performed a quality assessment of VLBI observations during CONT14. The radio sources and the VLBI stations that took part in the CONT14 sessions were analyzed according to their sensitivity levels. Furthermore, a robustness analysis was applied for the antennas.

The controllability of one station through the other stations can be investigated by the sensitivity analysis. The location of the station in the network and the total weights of its observations are the most important contributors for the sensitivity. On the other hand, the total observation number of a radio source, and the quality of the observations are also important for the sensitivity levels of the radio sources. It was also found that the investigation of the relationship between the structure of radio source and their sensitivity level is of interest.

According to the robustness analysis of the station coordinates, all of the stations are robust against undetectable gross errors. Some of the stations such as FORTLEZA, WESTFORD, and TSUKUB32 have significantly worse robustness in comparison to the other stations. It is possible that the worst robustness values can be due to the effects of the atmosphere that changes very much with time and with the location of the stations. Another explanation could be the remoteness of the station in the network.

Author Contributions: Analyzing and writing—original draft preparation, P.K.N.; review and editing, R.H., H.S., S.G., S.L., N.M., K.B., H.K., E.T.K. All authors have read and agreed to the published version of the manuscript.

Funding: This research received no external funding.

Acknowledgments: Pakize Küreç Nehbit acknowledges the Scientific and Technological Research Council of Turkey (TÜBİTAK) for the financial support of the post-doctoral research program (2219). The International VLBI Service for Geodesy and Astrometry (IVS), [2] and [32], are acknowledged for providing data used within this study. We would like to thank all reviewers for the detailed comments which helped to improve the manuscript.

Conflicts of Interest: The authors declare no conflict of interest.

References

1. GFZ VLBI Group. Available online: https://www.gfz-potsdam.de/en/section/space-geodetic-techniques/topics/geodetic-and-astrometric-vlbi/ (accessed on 2 March 2020).
2. Schuh, H.; Behrend, D. VLBI: A fascinating technique for geodesy and astrometry. *J. Geodyn*. **2012**, *61*, 68–80, doi:10.1016/j.jog.2012.07.007.
3. Heinkelmann, R.; Schuh, H. Very long baseline interferometry: Accuracy limits and relativistic tests. *Proc. Int. Astron. Union* **2009**, *5*, 286–290, doi:10.1017/S1743921309990524.
4. Shapiro, I.I. New Method for the Detection of Light Deflection by Solar Gravity. *Science* **1967**, *157*, 806–808.
5. Even-Tzur, G. Sensitivity Design for Monitoring Deformation Networks. *Boll. Geod. Sci. Affin.* **1999**, *54*, 313–324.
6. Hsu, R.; Hsiao, K. Pre-Computing the Sensitivity of a GPS station for crustal deformation monitoring. *J. Chin. Inst. Eng*. **2002**, *25*, 715–722.
7. Even-Tzur, G. Datum Definition and Its Influence on the Sensitivity of Geodetic Monitoring Networks. In Proceedings of the 12th FIG Symposium, Baden, Austria, 22–24 May 2006.
8. Küreç, P.; Konak, H. A priori sensitivity analysis for densification GPS networks and their capacities of crustal deformation monitoring: A real GPS network application. *Nat. Hazards Earth Syst. Sci*. **2014**, *14*, 1299–1308.
9. Konak, H.; Küreç Nehbit, P.; İnce, C.D. Determination of experimental sensitivity capacities against crustal movements of dense-geodetic networks: A real GPS network application. *Arab. J. Geosci*. **2019**, *12*, 596.
10. Vanicek, P.; Krakiwsky, E.J.; Craymer, M.R.; Gao, Y.; Ong, P.S. *Robustness Analysis*, *Final Contract Report*; 156; Department of Surveying Engineering Technical Report, University of New Brunswick: Fredericton, NB, Canada, 1990.
11. Baarda, W. Reliability and precision of networks. In Proceedings of the VII International Course for Engineering Surveys of High Precision, Darmstadt, Germany, 29 September–8 October 1976.
12. Kuang, S. Optimization and Design of Deformation Monitoring Schemes. Ph.D. Thesis, Department of Surveying Engineering Technical Report, University of New Brunswick, Fredericton, NB, Canada, 1991.
13. Berber, M. Robustness Analysis of Geodetic Networks. Ph.D. Thesis, University of Brunswick, Fredericton, NB, Canada, 2006.
14. Küreç Nehbit, P. A Continuous Strain Monitoring and Quality Assessment Strategy for GPS/GNSS Networks. Ph.D. Thesis, University of Kocaeli, Kocaeli, Turkey, 2018.
15. Nilsson, T.; Soja, B.; Karbon, M.; Heinkelmann, R.; Schuh, H. Application of Kalman filtering in VLBI data analysis. *Earth Planets Space* **2015**, *67*, 1–9, doi:10.1186/s40623-015-0307-y.
16. Böhm, J.; Böhm, S.; Nilsson, T.; Pany, A.; Plank, L.; Spicakova, H.; Teke, K.; Schuh, H. The New Vienna VLBI Software VieVS. In *Geodesy for Planet Earth*; International Association of Geodesy Symposia; Kenyon, S., Pacino, M., Marti, U., Eds.; Springer: Berlin/Heidelberg, 2012; Volume 136, doi:10.1007/978-3-642-20338-1_126.
17. Bardaa, W. *A Testing Procedure for Use in Geodetic Networks*; Netherlands Geodetic Commission, Publications on Geodesy, Computing Centre of the Delft Geodetic Institute: Delft, The Netherlands, 1968; Volume 2.

18. Aydin, C.; Demirel, H. Computation of Baarda's lower bound of the non-centrality parameter. *J. Geod*. **2004**, *78*, 437–441, doi:10.1007/s00190-004-0406-1.
19. Nothnagel, A. Very Long Baseline Interferometry. In *Handbuch der Geodäsie*, *1–58*; Springer Reference Naturwissenschaften Book Series; Freeden, W., Rummel, R., Eds.; Springer Spektrum: Berlin/Heidelberg, Germany, 2018, doi:10.1007/978-3-662-46900-2_110-1.
20. Teke, K. Sub-Daily Parameter Estimation in VLBI Data Analysis. Ph.D. Thesis, Institute of Geodesy and Geophysics, Vienna University of Technology, Vienna, Austria, 2011; p. 149, ISSN: 1811-8380.
21. Vanicek, P.; Craymer, M.R.; Krakiwsky, E.J. Robustness analysis of geodetic horizontal networks. *J. Geod*. **2001**, *75*, 199–209.
22. Küreç Nehbit, P.; Konak, H. The global and local robustness analysis in geodetic networks. *Int. J. Eng. Geosci*. **2020**, *5*, 42–48.
23. Wolf, P.R.; Ghilani, C.D. *Adjustment Computations: Statistics and Least Squares in Surveying and GIS*; John Wiley and Sons, Inc.: Hoboken, NJ, USA, 1997.
24. Baarda, W. Measures for the accuracy of geodetic networks. In Proceedings of the Symposium on Optimization of Design and Computation of Control Networks, Sopron, Hungary, 4–10 July 1977; pp. 419–436.
25. Öztürk, E.; Serbetçi, M. *Adjustment Volume 3*; Technical University of Karadeniz, Trabzon, Turkey, 1992.
26. Yalçınkaya, M.; Teke, K. Optimization of GPS networks with respect to accuracy and reliability criteria. In Proceedings of the 12th FIG Symposium, Baden, Austria, 22–24 May 2006.
27. Pelzer, H. *Geodaetische Netze in Landes- und Ingenieurvermessung II: Vortraege des Kontaktstudiums Februar 1985 in Hannover*, Wittwer: Stuttgart, Germany, 1985.
28. Xu, M.H.; Anderson, J.M.; Heinkelmann, R.; Lunz, S.; Schuh, H.; Wang, G.L. Structure effects for 3417 Celestial Reference Frame radio sources. *Astrophys. J. Suppl. Ser*. **2019**, *242*, 5.
29. Charlot, P. Radio source structure in Astrometric and geodetic very long baseline interferometry. *Astron. J.* **1990**, *99*, 1309.
30. Fey, A.L.; Charlot, P. VLBA observations of radio reference frame sources. II. Astrometric suitability based on observed structure. *Astrophys. J. Suppl. Ser.* **1997**, *111*, 95–142.
31. Anderson, J.M.; Xu, M.H. Source structure and measurement noise are as important as all other residual sources in geodetic VLBI combined. *J. Geophys. Res. Solid Earth* **2018**, *123*, 10–162, doi:10.1029/2018JB015550.
32. Nothnagel, A.; Artz, T.; Behrend, D.; Malkin, Z. International VLBI service for Geodesy and Astrometry—Delivering high-quality products and embarking on observations of the next generation. *J. Geod* **2017**, *91*, 711–721, doi:10.1007/s00190-016-0950-5.